RSC Advances

ROYAL SOCIETY OF CHEMISTRY

www.rsc.org/advances

RSC Advances

ARTICLE

Electrochemical reduction of carbon dioxide to formate with a Sn cathode and an $Ir_xSn_yRu_zO_2$/Ti anode

Received 00th January 20xx,
Accepted 00th January 20xx

DOI: 10.1039/x0xx00000x

www.rsc.org/

Rui Zhang,[a] Weixin Lv,[b] Guanghua Li,[a] Mohammed Adnan Mezaal[a] and Lixu Lei*[a]

Electrochemical reduction of CO_2 to formate has been studied extensively, and its most studies have focused on the faradaic efficiency for producing formate. However, the energy efficiency is also critical for possible industrialization of the process, as it specifies the energy recovered in the product. Here, we report that the energy efficiency is 35.6% when a Pt electrode is used as the anode, and it can increase to 42.1% when an $Ir_xSn_yRu_zO_2$/Ti electrode with lower overpotential for oxygen evolution reaction is used as the anode, in spite of their faradaic efficiencies for producing formate are very close (85.1% and 84.8%). When the $Ir_xSn_yRu_zO_2$/Ti electrode coated with Nafion membrane is used as the anode, the faradaic efficiency can maintain at 79.6% through a long time electrolysis of CO_2 for 500 C.

Introduction

In the past decades, a significant increase in CO_2 emission has occurred due to the industrial combustion of fossil fuels.[1] To reduce our dependence on the fossil fuel, renewable energy sources, such as solar and wind energies, are growing up rapidly. These renewable energies are difficult to be merged into the electricity grid due to their intermittent nature, therefore, their further expansion is highly limited by the availability of efficient energy storage and conversion techniques.[2] Electrochemical reduction of CO_2 to fuels and chemical feedstocks, powered by renewable electricity,[3, 4] is an attractive route for simultaneous elimination of CO_2 and storage of renewable energy.[5, 6]

Fig. 1 shows the evolution of publications on electrochemical reduction of CO_2 since the year of 1980 (Sources: Web of science, Thomson Reuters). Over the past few years and especially from the year of 2009, the research on electrochemical reduction of CO_2 has received much attention. To date, various products have been prepared by this way, including formic acid, carbon monoxide, methanol, ethanol and oxalic acid, etc.[7-16] Among them, formic acid or formate (depending on pH) is very attractive because it is a liquid of easy treatment and can be produced in high faradaic efficiency (typically > 80%).[12, 17-19] It is also a fundamental chemical which is widely used in the textile, tanning, rubber processing and pharmaceutical industries.[20] Formic acid could also function as an energy material, as it can be used in direct formic acid fuel cell to produce electricity.[21, 22]

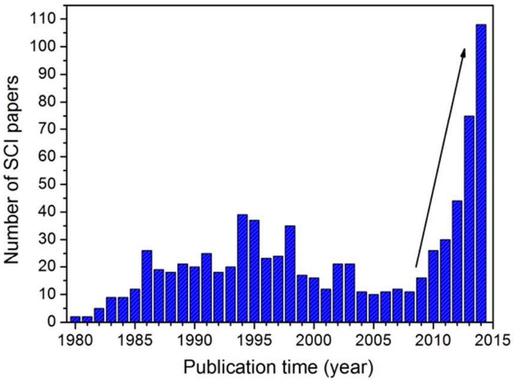

Fig. 1 Numbers of publications dedicated to the research of electrochemical reduction of CO_2 since the year of 1980.

However, to employ the electrochemical reduction of CO_2 as an energy reservoir, the energy efficiency of the process must be examined. To increase the energy efficiency, it has to decrease the overpotential on each electrode.[23] To date, only a few researchers focus on the research of the energy efficiency for electrochemical reduction of CO_2 to formate. Whipple *et al.* designed a microfluidic reactor with a continuous flowing electrolyte for electrochemical reduction of CO_2, it can achieve a faradaic efficiency of ~90% and an energy efficiency of 45% for formate production on Sn based gas diffusion electrode by using 0.5 mol L^{-1} KCl aqueous solution (pH=4) as the electrolyte.[24] Hori reported that the energy efficiency of electrochemical reduction of CO_2 to useful products would be roughly 30% to 40% under mild conditions.[25]

Our previous work found that the faradaic efficiency for producing formate can reach 91% when the accumulated concentration of formate in electrolyte is less than 0.01 mol L^{-1};[26] but it does not involve a study of energy efficiency. In this paper, we

---

[a] *School of Chemistry and Chemical Engineering, Southeast University, Nanjing 211189, PR China. E-mail: lixu.lei@seu.edu.cn; Tel: +86-25-5209 0620-6421*
[b] *School of Chemistry and Chemical Engineering, Yancheng Institute of Technology, Yancheng 224051, PR China*

concern the energy efficiency of the reaction. In this process, the reduction reaction of CO_2 occurs on the cathode and the oxidation reaction of H_2O occurs on the anode.[27]

Most researchers used Pt as the anode in the research of electrochemical reduction of CO_2, whereas the Pt electrode has high overpotential for oxygen evolution reaction (OER).[28] A lot of studies have shown that the most efficient electrocatalysts for OER are noble metals and their oxides. The oxides are more stable than pure metals because they cannot be further oxidized. Ruthenium oxide (RuO_2) is the most active catalyst but its activity is not sufficient for long-term utilization due to the increase of ruthenium oxidation state.[29] Conversely, iridium oxide (IrO_2) is stable and has also interesting catalytic properties for OER.[28] Out of these, SnO_2 can also be used as a catalyst for OER.[30, 31] In this paper, we utilized an $Ir_xSn_yRu_zO_2$/Ti anode to oxidize water. The study about using $Ir_xSn_yRu_zO_2$/Ti electrode as anode in electrochemical reduction of CO_2 has not reported before.

Experimental

Chemicals and Materials

Potassium bicarbonate (≥ 99.5%) was purchased from Sinopharm Chemical Reagent Co, Ltd (China). Highly pure nitrogen (≥ 99.99%) and carbon dioxide (≥ 99.99%) were supplied by Nanjing Spring Industrial Gas Plant (China). Tin plate (99.99%, 0.5 mm thickness) and Pt plate (99.99%) were purchased commercially. $Ir_xSn_yRu_zO_2$/Ti plate was purchased from Baoji Yichen Co. (China).

Electrochemical experiments

All the electrochemical experiments were carried out in an airtight and undivided glass cell equipped with a gas inlet and outlet which is able to pass the gas through the solution. A conventional three-electrode system was used during the experiments. The working electrode was a Sn plate. A Pt plate (2 cm^2) or an $Ir_xSn_yRu_zO_2$/Ti plate (2 cm^2) was chosen as the counter electrode and an Ag/AgCl electrode in saturated KCl was used as the reference electrode. All experiments were performed under ambient pressure and at room temperature (25 ± 2.5 °C).

All the electrochemical measurements were performed with a CS350 electrochemical workstation (Wuhan CorrTest Instrument Co., Ltd., China). Cyclic voltammetry (CV) were performed in 40 mL of 0.1 mol L^{-1} $KHCO_3$ solution at a scan rate of 0.05 V s^{-1}. To reveal the true energy input required for this process, the CV was recorded in two-electrode mode (Sn cathode, Pt or $Ir_xSn_yRu_zO_2$/Ti anode), which was denoted as Sn−Pt or Sn−$Ir_xSn_yRu_zO_2$/Ti. The current density (j) is determined on the geometrical area of the electrode.

Electrolysis was performed potentiostatically by holding the cathode potential at −1.8 V vs. Ag/AgCl using a LAND CT2001C cell performance-testing instrument (Wuhan Electronics Co., Ltd., China). The electrolyte used was 40 mL of 0.1 mol L^{-1} $KHCO_3$ aqueous solution, and was saturated with CO_2 before each electrolysis process. CO_2 gas was continuously aerated at a flow rate of 10 mL min^{-1} during the electrolysis process. The electrolysis experiments were terminated when the total charge passed reached 50 C.

Analysis and calculations

Scanning electron microscope (SEM) images were taken with a Hitachi S-4800 microscope at an acceleration voltage of 15 kV. X-ray diffraction pattern (XRD) was recorded on a Rigaku D/MAX 2200 diffractometer using Cu Kα radiation (λ = 1.54056 Å), scan range from 20 to 80 ° at a scan rate of 0.12 ° s^{-1}.

Formate produced in the electrolyte during the electrolysis was directly analyzed by ion chromatography (ICS-900 Dionex). The column was an IonPac AS11-HC anionic column using 0.02 mol L^{-1} KOH as the mobile phase at the rate of 1 mL min^{-1}. 10 µL of the electrolyte were used for each time.

The faradaic efficiency for the formation of formate (f) is calculated as follows:

$$f = 2n\mathrm{F} / Q \qquad (1)$$

where 2 represents the number of electrons required for the formation of one molecule of formate from CO_2; n is the moles of the formate produced; F is Faraday's constant (96485 C mol^{-1} of electrons); and Q is the total charge in Coulomb passed across the electrode during the electrolysis.

The energy efficiency is a key factor in determining the economic feasibility of converting CO_2 to fuels by utilizing electricity.[32] The energy efficiency for electrochemical reduction of CO_2 to formate is calculated as follows:

$$\text{Energy efficiency} = E^{\circ} f / \text{Applied cell potential} \qquad (2)$$

where E° represents the standard electromotive force of the cell, E° is −1.43 V in this work.

Results and discussion

Fig. 2 shows the SEM image and the EDS spectrum of the $Ir_xSn_yRu_zO_2$/Ti electrode. It can be seen that the surface of the $Ir_xSn_yRu_zO_2$/Ti electrode is coarse, since the electrode base is Ti plate and covered by the oxides of Ru, Sn and Ir. From the EDS spectrum, it can be seen that the atomic percents of Ru, Sn and Ir are 8.71%, 3.83% and 1.29%, respectively.

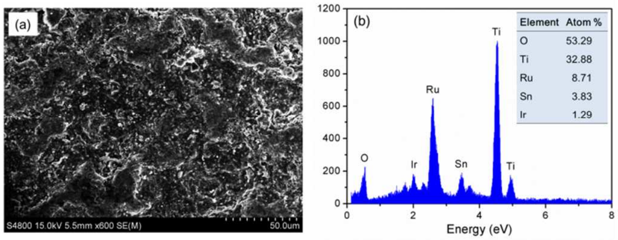

Fig. 2 SEM image (a) and EDS spectrum (b) of the surface of the $Ir_xSn_yRu_zO_2$/Ti electrode.

Structural characterization of the $Ir_xSn_yRu_zO_2$/Ti electrode was performed by XRD analysis, which is shown in Fig. 3. It shows the (100), (002), (101), (102), (110), (103), (112) and (201) diffraction peaks of Ti together with the (110), (101), and (211) peaks of RuO_2.

No diffraction peaks for SnO_2 and IrO_2 can be observed because of the low contents of SnO_2 and IrO_2 in the surface of $Ir_xSn_yRu_zO_2$/Ti electrode.

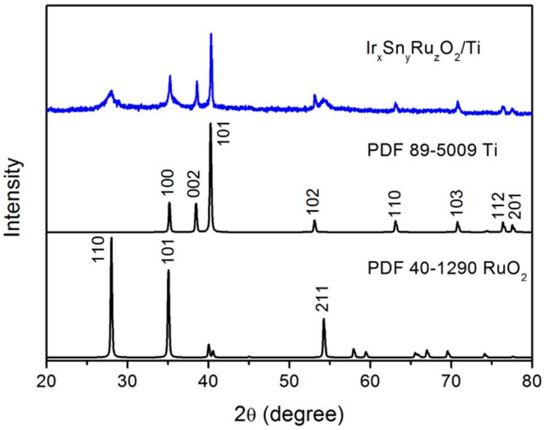

Fig. 3 XRD pattern of the surface of the $Ir_xSn_yRu_zO_2$/Ti electrode.

The anode reaction for electrochemical reduction of CO_2 is OER, which is shown in Eq. (3):

$$2H_2O = O_2 + 4H^+ + 4e^- \qquad (3)$$

The electrochemical activities of the Pt electrode and the $Ir_xSn_yRu_zO_2$/Ti electrode towards OER were studied using CV technique. It can be seen from Fig. 4 that the Pt electrode shows poor catalytic activity for OER compared with the $Ir_xSn_yRu_zO_2$/Ti electrode. The $Ir_xSn_yRu_zO_2$/Ti electrode produces nearly rectangular curves when the potential sweep range is from 0 to 1.0 V vs. Ag/AgCl, indicating that the $Ir_xSn_yRu_zO_2$/Ti electrode has capacitive behavior. The oxidation current density of the OER on Pt electrode at 1.8 V vs. Ag/AgCl is 0.55 mA cm^{-2}. At the same current density, the potential of $Ir_xSn_yRu_zO_2$/Ti electrode is around 1.3 V vs. Ag/AgCl.

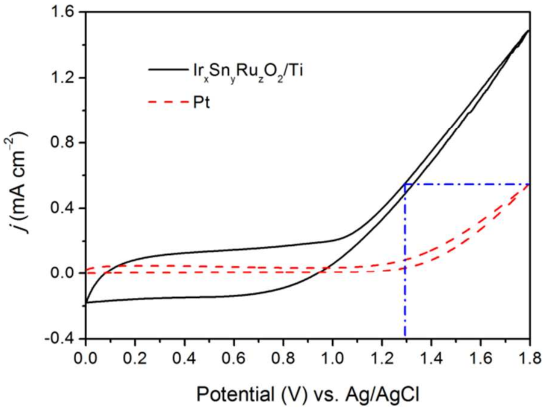

Fig. 4 CV curves of OER on the Pt electrode and the $Ir_xSn_yRu_zO_2$/Ti electrode.

Following our previous work,[26] the electrochemical reduction of CO_2 was carried out at the found optimal electrolysis conditions, that is, the electrolysis potential was −1.8 V vs. Ag/AgCl and the concentration of the $KHCO_3$ aqueous electrolyte was 0.1 mol L^{-1}. To calculate the energy efficiency, the value of applied cell potential is needed. So our work must investigate the appropriate applied cell potential between the cathode and the anode without reference electrode. The study of CV was carried out for this purpose, the working electrode is the Sn plate, and the counter electrode is the Pt electrode or the $Ir_xSn_yRu_zO_2$/Ti electrode, the reference electrode is the Ag/AgCl electrode. Firstly, we compared the CV curves shown in Fig. 5 when the anode was the Pt electrode or the $Ir_xSn_yRu_zO_2$/Ti electrode, and found that curve (a) is nearly the same with curve (b), the current density at −1.8 V vs. Ag/AgCl is around 3.5 mA cm^{-2}. Secondly, curves (c) and (d) are recorded in two-electrode mode (without reference electrode) for obtaining the true energy input required for this process, the terminal cell potentials of curves (c) and (d) stop at the same current density (3.5 mA cm^{-2}), and the values are 3.42 V and 2.88 V at 3.5 mA cm^{-2} as the anodes are Pt electrode and the $Ir_xSn_yRu_zO_2$/Ti electrode, respectively. It indicates that the applied cell potential is lower when the anode is the $Ir_xSn_yRu_zO_2$/Ti electrode. A pair of redox peaks is observed for all the CV curves which can be attributed to the formation and the reduction of tin oxides respectively.[26]

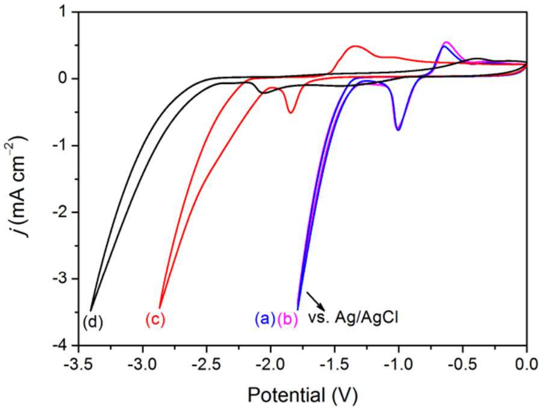

Fig. 5 CV curves on a Sn electrode with an $Ir_xSn_yRu_zO_2$/Ti electrode (a) or a Pt electrode (b) as counter electrode and an Ag/AgCl electrode as reference electrode for electrochemical reduction of CO_2. CV curves on a Sn electrode with an $Ir_xSn_yRu_zO_2$/Ti electrode (c) or a Pt electrode (d) as counter electrode for electrochemical reduction of CO_2 recorded in two-electrode mode. The measurements were performed in 0.1 mol L^{-1} $KHCO_3$ solutions after being bubbled with CO_2 for 30 min.

Fig. 6 is the current density curves for electrochemical reduction of CO_2 on Sn cathode at different cell potentials when the Pt electrode or the $Ir_xSn_yRu_zO_2$/Ti electrode is used as the anode. Several adjacent cell potentials are selected in this experiment, the cell potential range is from 3.02 to 3.62 V for the Pt anode, and is from 2.48 to 3.08 V for the $Ir_xSn_yRu_zO_2$/Ti anode. For the Pt anode and the $Ir_xSn_yRu_zO_2$/Ti anode, each cell potential for the former is 0.54 V higher than that for the latter, and their current densities are nearly the same.

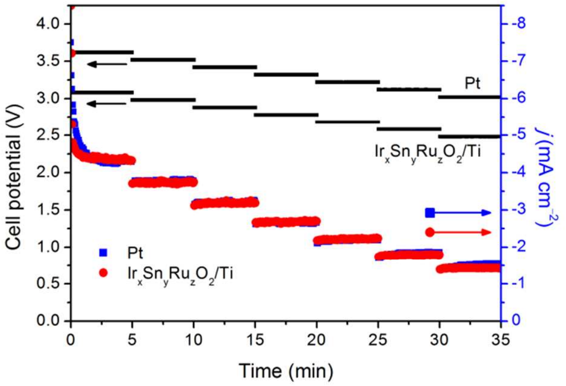

Fig. 6 Current densities at different cell potentials when use the Pt electrode or the $Ir_xSn_yRu_zO_2$/Ti electrode as anode during the electrochemical reduction of CO_2 in 0.1 mol L^{-1} $KHCO_3$ solution.

In this work, we hope to use an activated anode to lower the overpotential for OER. It can be seen from the CV measurements (Fig. 4 and Fig. 5) that, the $Ir_xSn_yRu_zO_2$/Ti electrode shows excellent catalytic activity for OER than the Pt electrode, which may improve the energy efficiency of the whole reaction for electrochemical reduction of CO_2. Fig. 7 is the qualitative reaction scheme for OER on the Pt anode or the $Ir_xSn_yRu_zO_2$/Ti anode from the above experiments. The overpotential for OER on Pt electrode (η_1) is obviously higher than that on $Ir_xSn_yRu_zO_2$/Ti electrode (η_2). From the analysis results of Fig. 5 and Fig. 6, it can be obtained that the value of ($\eta_1 - \eta_2$) is 0.54 V.

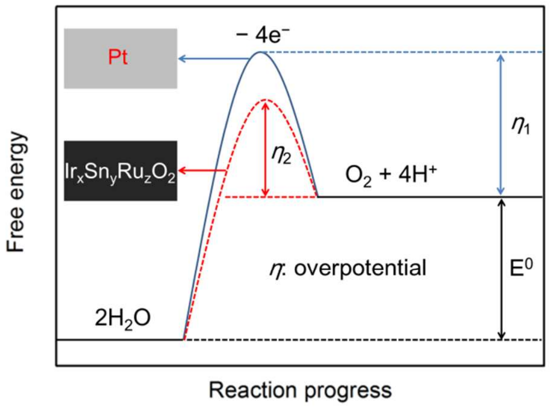

Fig. 7 Qualitative reaction scheme for OER on Pt anode or $Ir_xSn_yRu_zO_2$/Ti anode.

Low overpotential is helpful for increasing the energy efficiency for electrochemical reduction of CO_2. The energy efficiency is a key factor in determining the economic feasibility of converting CO_2 to fuels by utilizing electricity. The energy efficiency for producing formate was calculated using Eq. (2), as shown in Fig. 7 where the apparent standard electromotive force of the cell, E° is −1.43 V,[24] as predicted by Nernst equation. For evaluating the energy efficiency, the electrolysis experiments were carried out at different applied cell potentials.

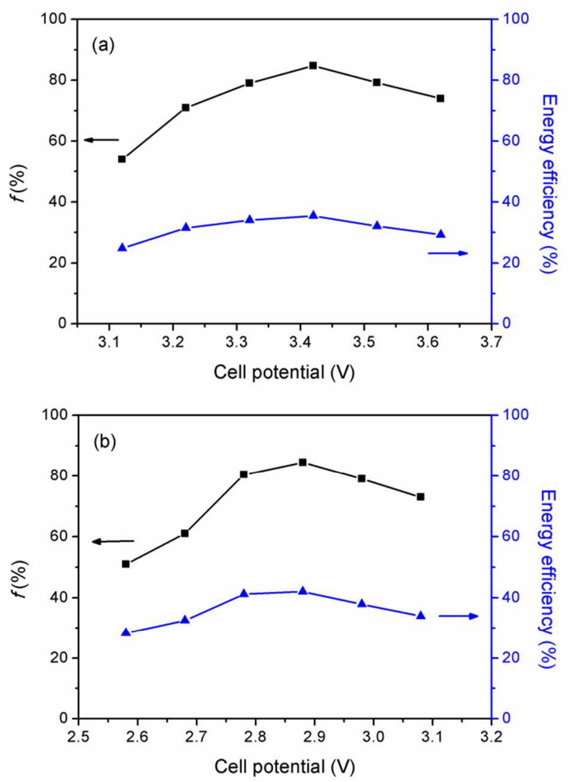

Fig. 8 Variations of energy efficiency and faradaic efficiency for producing formate on the Sn electrode with the applied potential when using the Pt electrode (a) or the $Ir_xSn_yRu_zO_2$/Ti electrode (b) as the anode.

In our previous work, the optimal potential for electrochemical reduction of CO_2 was −1.8 V vs. Ag/AgCl. The corresponding applied cell potentials of Sn−Pt and Sn−$Ir_xSn_yRu_zO_2$/Ti are 3.42 V and 2.88 V, respectively. Several adjacent cell potentials are selected in this experiment to confirm an optimal electrolysis condition, it can be seen from Fig. 8 that the highest faradaic efficiency for Sn−Pt is 85.1% obtained at 3.42 V (Fig. 8a), and that for Sn−$Ir_xSn_yRu_zO_2$/Ti is 84.8% obtained at 2.88 V (Fig. 8b). Although their faradaic efficiencies are very close, the energy efficiency of the Sn−$Ir_xSn_yRu_zO_2$/Ti (42.1%) is higher than that of the Sn−Pt (35.6%) because of the lower overpotential for OER on the $Ir_xSn_yRu_zO_2$/Ti electrode. It’s worth mentioning that the

$Ir_xSn_yRu_zO_2$/Ti electrode can not only be used for producing formate, but also can be used for producing other products (such as CO, methanol or hydrocarbons) with less energy input.

For evaluate the stability of the $Ir_xSn_yRu_zO_2$/Ti electrode, a long time electrolysis experiment is required. In this experiment, the products of formate will be re-oxidization on the anode if the concentration of formate is high. In order to avoid the formate oxidation on the anode, H-type cell divided by a nafion membrane was used by some researchers. Whereas, the H-type cell may not be a good choice in this experiment. Narayanan *et al.* used In and Pb powders as the catalysts for electrochemical reduction of CO_2 to formate in a H-type cell. They found that the faradaic efficiency for producing formate in 1 mol L^{-1} $NaHCO_3$ solution was as high as 80% after 300 s; however, the faradaic efficiency began to decline over a period of 1 h. They thought that the decrease of the faradaic efficiency during continuous operation was a result of the buildup of diffusion barriers resulting in the reduced availability of CO_2 for reduction at the surface of the electrode.[33] We have found another effective method for retarding the oxidation of formate in our previous work, that is coating a Nafion membrane on the anode.[18]

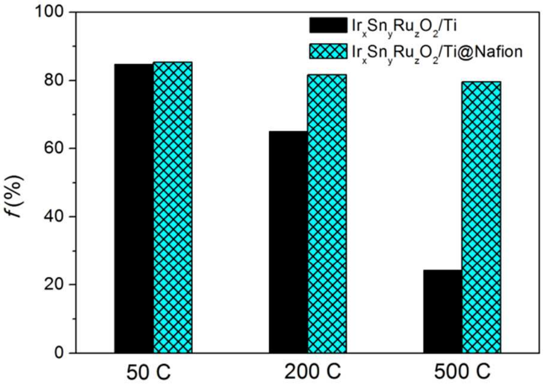

Fig. 9 Variations in faradaic efficiency for producing formate with the charge passed when the anode is $Ir_xSn_yRu_zO_2$/Ti or $Ir_xSn_yRu_zO_2$/Ti@Nafion electrode.

In this paper, we also performed long time electrolysis experiment using $Ir_xSn_yRu_zO_2$/Ti electrode coated with Nafion membrane as the anode which is prepared by immersing the electrode into 5 wt.% Nafion solution. As shown in Fig. 9, the faradaic efficiency decreases from 85.3% to 79.6% as the charge passed increases from 50 to 500 C. However, when a naked $Ir_xSn_yRu_zO_2$/Ti electrode is used as the anode, the faradaic efficiency decreases significantly from 84.8% to 29.3% as the charge passed increases from 50 to 500 C (Fig. 9).

Curves (a) and (c) in Fig. 10 show the CV curves on the $Ir_xSn_yRu_zO_2$/Ti electrodes with and without Nafion membrane in the $KHCO_3$ electrolytes, respectively. It can be seen that the current density on the naked $Ir_xSn_yRu_zO_2$/Ti electrode is nearly the same with that on the $Ir_xSn_yRu_zO_2$/Ti electrode coated with Nafion membrane. Therefore, the Nafion coat has negligible effect on OER. Curves (b) and (d) in Fig. 10 show the CV curves on the $Ir_xSn_yRu_zO_2$/Ti electrodes with and without Nafion membrane in $KHCO_3$ electrolytes containing 0.05 mol L^{-1} potassium formate, respectively. The current density on $Ir_xSn_yRu_zO_2$/Ti electrode coated with Nafion membrane is obviously lower than that on the naked $Ir_xSn_yRu_zO_2$/Ti electrode if the electrolyte contains $HCOO^-$. These results reveal that the Nafion membrane can effectively retard the oxidation of formate on $Ir_xSn_yRu_zO_2$/Ti anode.

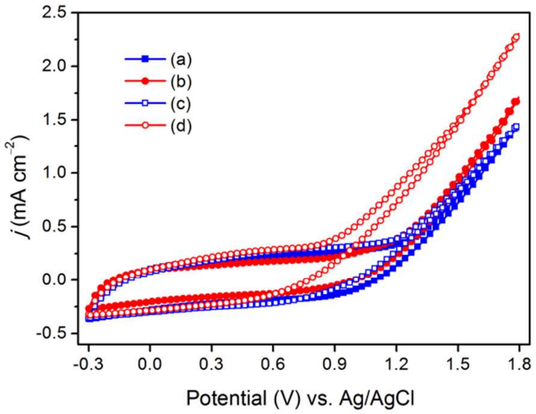

Fig. 10 CV curves on the $Ir_xSn_yRu_zO_2$/Ti electrode with (a) or without (c) Nafion membrane in electrolytes and CV curves on the $Ir_xSn_yRu_zO_2$/Ti electrode with (b) or without (d) Nafion membrane in electrolytes containing 0.05 mol L^{-1} $HCOO^-$. The measurements were performed in 0.1 mol L^{-1} $KHCO_3$ electrolyte after being bubbled with CO_2 for 30 min.

Conclusions

The $Ir_xSn_yRu_zO_2$/Ti anode shows better catalytic activity for OER than the Pt anode. At the same current density of 3.5 mA cm^{-2}, the applied cell potentials for Sn−$Ir_xSn_yRu_zO_2$/Ti and Sn−Pt are 2.88 and 3.42 V, respectively. The electrode with excellent catalytic activity for OER used in electrochemical reduction of CO_2 can increase the energy efficiency of the whole reaction. In this paper, the energy efficiency of the Sn−$Ir_xSn_yRu_zO_2$/Ti (42.1%) is higher than that of the Sn−Pt (35.6%).

When the $Ir_xSn_yRu_zO_2$/Ti electrode coated with Nafion membrane is used as the anode, the faradaic efficiency decreases from 85.3% to 79.6% as the charge passed increases from 50 to 500 C; when a naked $Ir_xSn_yRu_zO_2$/Ti electrode is used as the anode, the faradaic efficiency decreases to 24.3% as the charge passed increases to 500 C. It indicates that the Nafion membrane on $Ir_xSn_yRu_zO_2$/Ti anode can effectively retard the oxidation of formate.

Acknowledgements

This work is supported by the Department of Science and Technology, Jiangsu Province (BY2013073-03), the Department of Education for the Fundamental Research Funds for the Central Universities, Jiangsu Province for the College graduate research and innovation projects (CXLX13_086).

References

1 T. R. Karl and K. E. Trenberth, *Science*, 2003, **302**, 1719-1723.
2 X. Luo, J. H. Wang, M. Dooner and J. Clarke, *Appl. Energ.*, 2015, **137**, 511-536.
3 D. F. Gao, H. Zhou, J. Wang, S. Miao, F. Yang, G. Wang, J. Wang and X. Bao, *J. Am. Chem. Soc.*, 2015, **137**, 4288-4291.
4 C. W. Machan, S. A. Chabolla, J. Yin, M. K. Gilson, F. A. Tezcan and C. P. Kubiak, *J. Am. Chem. Soc.*, 2014, **136**, 14598-14607.
5 C. H. Lee and M. W. Kanan, *ACS Catal.*, 2014, **5**, 465-469.
6 R. Zhang, W. X. Lv, G. H. Li and L. X. Lei, *Mater. Lett.*, 2015, **141**, 63-66.
7 V. S. K. Yadav and M. K. Purkait, *RSC Adv.*, 2015, **5**, 40414-40421.
8 E. Barton Cole, P. S. Lakkaraju, D. M. Rampulla, A. J. Morris, E. Abelev and A. B. Bocarsly, *J. Am. Chem. Soc.*, 2010, **132**, 11539-11551.
9 Y. Chen, C. W. Li and M. W. Kanan, *J. Am. Chem. Soc.*, 2012, **134**, 19969-19972.
10 R. Angamuthu, P. Byers, M. Lutz, A. L. Spek and E. Bouwman, *Science*, 2010, **327**, 313-315.
11 X. Lu, D. Y. C. Leung, H. Wang, M. K. H. Leung and J. Xuan, *ChemElectroChem*, 2014, **1**, 836-849.
12 Q. N. Wang, H. Dong, H. Yu and H. B. Yu, *J. Power Sources*, 2015, **279**, 1-5.
13 Q. N. Wang, H. Dong and H. B. Yu, *J. Power Sources*, 2014, **271**, 278-284.
14 H. Z. Zhao, Y. Zhang, Y. Y. Chang and Z. S. Li, *J. Power Sources*, 2012, **217**, 59-64.
15 W. X. Lv, R. Zhang, P. R. Gao, C. X. Gong and L. X. Lei, *J. Solid State Electrochem.*, 2013, **17**, 2789-2794.
16 D. H. Chi, H. P. Yang, Y. F. Du, T. Lv, G. J. Sui, H. Wang and J. X. Lu, *RSC Adv.*, 2014, **4**, 37329-37332.
17 G. K. S. Prakash, F. A. Viva and G. A. Olah, *J. Power Sources*, 2013, **223**, 68-73.
18 R. Zhang, W. X. Lv, G. H. Li, M. A. Mezaal, X. J. Li and L. X. Lei, *J. Power Sources*, 2014, **272**, 303-310.
19 S. Zhang, P. Kang and T. J. Meyer, *J. Am. Chem. Soc.*, 2014, **136**, 1734-1737.
20 H. Uslu, C. Bayat, S. Goekmen and Y. Yorulmaz, *J. Chem. Eng. Data*, 2009, **54**, 48-53.
21 J. Yang, C. G. Tian, L. Wang and H. G. Fu, *J. Mater. Chem.*, 2011, **21**, 3384-3390.
22 J. F. Chang, L. G. Feng, C. P. Liu, W. Xing and X. L. Hu, *Angew. Chem. Int. Ed.*, 2014, **53**, 122-126.
23 D. T. Whipple and P. J. A. Kenis, *J. Phys. Chem. Lett.*, 2010, **1**, 3451-3458.
24 D. T. Whipple, E. C. Finke and P. J. A. Kenis, *Electrochem. Solid St.*, 2010, **13**, B109-B111.
25 Y. Hori, *Electrochemical CO$_2$ Reduction on Metal Electrodes*, Springer, Modern Aspects of Electrochemistry, 2008.
26 W. X. Lv, R. Zhang, P. R. Gao and L. X. Lei, *J. Power Sources*, 2014, **253**, 276-281.
27 J. J. Wu, F. G. Risalvato, P. P. Sharma, P. J. Pellechia, F. S. Ke and X. D. Zhou, *J. Electrochem Soc.*, 2013, **160**, F953-F957.
28 S. Y. Huang, P. Ganesan, H. Y. Jung and B. N. Popov, *J. Power Sources*, 2012, **198**, 23-29.
29 T. Audichon, E. Mayousse, S. Morisset, C. Morais, C. Comminges, T. W. Napporn and K. B. Kokoh, *Int. J. Hydrogen Energ.*, 2014, **39**, 16785-16796.
30 S. Ferro, D. Rosestolato, C. A. Martínez-Huitle and A. De Battisti, *Electrochim. Acta*, 2014, **146**, 257-261.
31 I. C. Gonçalves, W. T. P. dos Santos, D. V. Franco and L. M. Da Silva, *Electrochim. Acta*, 2014, **121**, 1-14.
32 B. A. Rosen, A. Salehi-Khojin, M. R. Thorson, W. Zhu, D. T. Whipple, P. J. A. Kenis and R. I. Masel, *Science*, 2011, **334**, 643-644.
33 S. R. Narayanan, B. Haines, J. Soler and T. I. Valdez, *J. Electrochem. Soc.*, 2011, **158**, A167-A173

Graphical Abstract

The energy efficiency for electrochemical reduction of CO_2 to formate is 35.6% when a Pt electrode is used as the anode, and it can increase to 42.1% when an $Ir_xSn_yRu_zO_2$/Ti electrode with lower overpotential for oxygen evolution reaction is used as the anode.